

Deployment of Long-measured Flexible Structure in Orbit

Alexandr E. ZAKRZHEVSKY
S. P. Timoshenko Institute of Mechanics NAS of Ukraine
3, Petra Nesterova Street, Kiev, Ukraine, 03057
alex.zakr@mail.ru

Abstract

Dynamics of the spacecraft with giro-gravitational system of stabilisation, in which the pantograph design deployed in an orbit and containing on the end the concentrated mass is used as the gravitational stabilizer and the carrier of solar batteries, is investigated. The analysis of the obtained information is carried out and graphs that illustrate behaviour of characteristic variables are discussed.

Keywords: Spacecraft, pantograph structure, deployment

1. Introduction

The deployment of spacecraft delivered into orbit in a compact form perturbs their attitude. The study of such transformed configurations is required for minimization of deployment duration, mass, and power resources, for analysis of the effect of such structures on the spacecraft attitude motion. There exist a large number of studies in the literature dedicated to the deployment of elastic appendages of different shape from the fixed basis as well as from a rotating SC. A short review of these publications is contained in [1].

Works, except for work [2], which would investigate the dynamics of deployment in orbit of pantograph designs, are unknown to the author. This research generalises the work [2] by the additional account of transversal displacements of the deployed pantograph design with objective to study their effect on the dynamics of the SC and its elements.

2. Physical model of system

Here the SC that includes the gyro-gravitational system of stabilization is studied during the deployment of the flexible pantograph structure according to the program motion into the elongated flexible gravitational stabilizer (GS). It serves also as the carrier of solar batteries and tip mass. The SC includes two gyro-dampers (GD) which are installed for attitude stabilization. The SC is injected in a circular earth orbit with altitude 400 km. Basic elements of the SC are shown in Fig. (1). Here, element 1 is the SC main module, element 2 is the spatial structure that consists of two plain coupled pantographs, elements 3 and 4 represent the GD.

The deployment is initiated when the points joining each plain pantograph to the main module start to approach synchronously. The distance between these points in each pantograph is $b(t)$. The dynamics of the deployment actuating drive are not taken into

consideration here since this mechanism is very simple and may be realized as a device that has no effect on the SC dynamics.

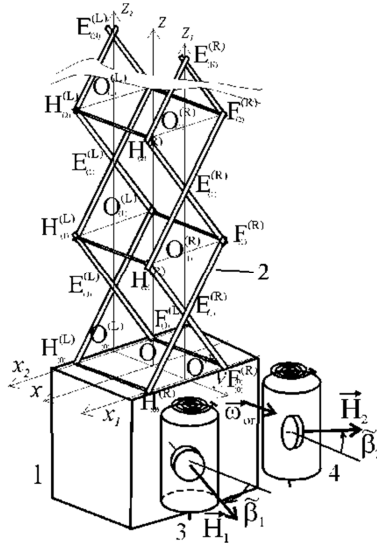


Figure 1. Basic elements of the spacecraft

The deployable structures possess considerable flexibility. Because of requirements to maintain the shape of the gravitational stabilizer, some restrictions must be imposed on the deployment and design parameters. They can be determined via the process of numerical simulations. The GD role in the process of deployment and after its completion is also studied further.

3. Mechanical model of system

The generalized mechanical model of the system under consideration may be represented as a main rigid body S_1 and body S_2 of variable configuration attached to it. The body S_1 is the gyro-static part and includes the GD, which do not change the rotational body inertia. The motion of the body S_1 is defined by the velocity vector \mathbf{v}_O of the point O and vector of absolute angular velocity $\boldsymbol{\omega}$.

The following frames of reference will be useful for the problem statement: \overline{CXYZ} is an earth-centered inertial reference frame; $Oxyz$ is the body S_1 fixed reference frame (Figure 1) with Oz along the design position of the GS axis; the orbital frame of reference $Ox'oy'oz'$ is fixed in the SC mass centre. These frames are introduced in such a way as in Ref. [3].

The position vector \mathbf{r} defines the location of the arbitrary point P with respect to the reference frame \overline{CXYZ} , and the position vector \mathbf{r}' – with respect to the reference frame $Oxyz$. In contrast to the problem of the relative motion of attached bodies described by

Lurie [5], here one has the more general case when the expression for \mathbf{r}' depends on time t explicitly, and not only through the generalized coordinates:

$$\mathbf{r}' = \mathbf{r}'(q_1, \dots, q_n, t) \tag{1}$$

As a result, \mathbf{r}' varies during deployment even in the absence of the relative elastic motion of the design.

Each of two pantographs is made of elastic rods in length $2a$ and mass $2m_d(i)$, where index i is used for the numbering of tiers that form full rhombuses. These rods are connected at the joints $E_{(i)}^{(R)}, E_{(i)}^{(L)}, (i = \overline{0, N})$, where N is the number of the tiers, and at points $H_{(i)}^{(R)}, H_{(i)}^{(L)}, F_{(i)}^{(R)}, F_{(i)}^{(L)}, (i = \overline{1, N})$, where the superscripts identify the pantograph as per Figure 1.

The pantograph structure has a compact form in the beginning (a transport condition). The inclination angles of the rods of all pantograph tiers with respect to axis Ox are equal to 5° . After deployment of the design, values of the specified angles reach 75° .

Elastic rods of the physical model have been replaced in the mechanical model by equivalent constructions of two rigid rods connected by the spring-bias cylindrical hinges with damping. Damping is used in order to approach the dynamics to reality at least in a qualitative sense. Stiffness of the springs in the hinges is defined from the condition of equal deflections of two constructions (Figure 2) under equal loads. The equivalent construction (in Figure 2 below) has the same deflection when spring resistance c_{joint} in the hinge is equal to $3EJ/(2a)$. Such a replacement is completely justified, as the configuration of the design is defined by mutual positions of the middle and end points of the rods. Besides, all dynamic values for the real design and its mechanical model at identical positions and velocities of mentioned above points with the same name are almost identical. It is applicable to the expressions for their tensor of inertia, moment of momentum, kinetic energy, and potential energy.

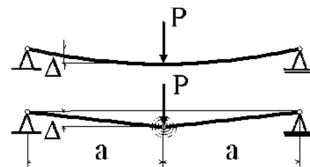


Figure 2. Beams with equivalent bending stiffness

4. Mathematical model of system

The equations of motion of the system under consideration become the most compact and convenient for numerical integration, if one chooses the instantaneous position of the mass centre C as an origin. Then one can obtain the following Lagrange's equations of the second kind for the generalized co-ordinates q_s :

$$E_s(T_r^0) - M \mathbf{r}_C^{**} \cdot \frac{\partial \mathbf{r}_C'}{\partial q_s} - \frac{1}{2} \boldsymbol{\omega} \cdot \frac{\partial \boldsymbol{\Theta}^C}{\partial q_s} \cdot \boldsymbol{\omega} + \dot{\boldsymbol{\omega}} \cdot \frac{\partial \mathbf{K}_r^C}{\partial \dot{q}_s} + \boldsymbol{\omega} \cdot E_s^*(\mathbf{K}_r^C) = Q_s \tag{2}$$

The equation of the attitude motion may be obtained as the Euler-Lagrange equation [4]

$$\mathbf{\Theta}^C \cdot \dot{\boldsymbol{\omega}} + \mathbf{\Theta}^C \cdot \boldsymbol{\omega} + \boldsymbol{\omega} \times (\mathbf{\Theta}^C \cdot \boldsymbol{\omega}) + \boldsymbol{\omega} \times \mathbf{K}_r^C = \mathbf{m}^C \quad (3)$$

The following notations are used here: $\mathbf{\Theta}^C$ is the inertia tensor of the whole system with respect to point C , $\mathbf{K}_r^C = \int_m \mathbf{r}' \times \mathbf{r}' dm - M \mathbf{r}_C' \times \mathbf{r}_C'$ is the relative moment of momentum of the deployed part with respect to point C ; \mathbf{r}_C' is position vector of the instant position of the mass centre C in the frame of reference $Oxyz$; the symbol $*$ denotes time differentiation in the reference frame $Oxyz$; M is the total mass of the system; T_r^O is the kinetic energy of the relative motion of the carried bodies calculated under condition of definition of relative velocities of their points with respect to O ; Q_s are generalized forces that take into account the elastic and dissipative characteristics of the construction; $E_j(\cdot) = \frac{d}{dt} \frac{\partial(\cdot)}{\partial \dot{q}_j} - \frac{\partial(\cdot)}{\partial q_j}$ is the Euler's operator; $E_j^*(\cdot) = \frac{\partial}{\partial t} \frac{\partial(\cdot)}{\partial \dot{q}_j} - \frac{\partial(\cdot)}{\partial q_j}$ is also the Euler's operator, but the time differentiation is performed in the reference frame $Oxyz$; \mathbf{m}^C is the gravitational torque; symbols \times and \cdot in Eqs. (2), (3) denote vector and scalar product respectively.

If to supplement Eqs. (2), (3) with the kinematical equations, one obtains a closed system of equations of motion. The parameters of Rodrigues-Hamilton were chosen as the attitude parameters [4]. Further, it is necessary to choose proper generalized co-ordinates q_s and determine expressions for \mathbf{r}_C' , $\mathbf{\Theta}^C$, T_r^C , \mathbf{K}_r^C , Π and all their derivatives with respect to time and generalized co-ordinates, which appear into expressions for factors of the equations (2), (3).

During deployment, Coriolis forces act on the material points because of the rotational-translational motion. These forces can produce deformations of an elastic structure in the transverse direction. At the same time, transverse forces are absent in the direction of the orbit binormal. Hence, the displacements of the design along the axis Oy can be neglected.

In this study, values of co-ordinates x_i, z_i ($i = \overline{1, N}$) of points E_i of each tier, lying on axis Oz on the straight lines connecting points $E_{(i)}^{(L)}, E_{(i)}^{(R)}$, and angles $\tilde{\beta}_k$ ($k=1,2$) (Figure 1) have been chosen as the generalized co-ordinates. (Note that $z_i = z_{i,p}(t) + z_{i,e}$, where $z_{i,p}(t)$ are prescribed functions of time and $z_{i,e}$ are independent variables). The pantograph structures having 20 tiers were studied.

The original computation package is developed for the numerical integration of the obtained ordinary differential equations in the frame of the Cauchy problem. The majority of operators of the program is obtained as Fortran-expressions in Mathematica5[®] in the codes written specifically for the system studied.

It is obvious that the dynamics of a complex flexible structure depend on the time history of the deployment. Two such time histories were used here. The deployment of space designs often used such a law $b(t)$ that the velocity time history of an actuating motor $\dot{b}(t)$ looks like the line 1 in Figure 3. Such a function $\dot{b}(t)$ has two angular points, and a function $\ddot{b}(t)$ (so and a function of an actuating force or torque) has four points of discontinuities. Action of such a force on an oscillating system brings additional perturbations in its dynamics.

Therefore, the alternative law of deployment of the design was considered. For this law $\ddot{b}(t)$ does not contain points of discontinuities. Such a law can be constructed using the solution of the optimal control problem (see [6], Special Case II). It brings essentially less perturbation in the dynamics of the system than the first one as the numerical simulations had shown.

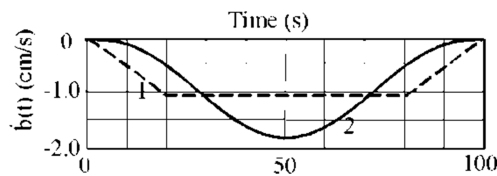


Figure 3. Laws of deployment

5. Numerical simulation

The torque of the central Newtonian field, corresponding to a circular orbit of 600 km altitude was considered as the external perturbing torque. Though the SC movement along an orbit is not considered here, the orbit parameters are used to calculate the gravitational torque and projections of the total SC moment of momentum to the inertial frame of reference. It is necessary for the monitoring of errors of the numerical integration of the initial value problem. Expressions governing the change of the total moment of momentum of the system are derived and numerically integrated along with the equations of motion for the system dynamics in order to identify mistakes in the code. The results agree within eight significant figures for each projection during monitoring.

Key system parameter values are: mass of main body $m_1 = 350$ kg, rods mass $m_1 = 1$ kg, bending stiffness $EJ = 20\text{--}80$ N m², decrement of oscillations $\vartheta = 0.001$, components of the main body inertia tensor $J_{xx} = 4000$ kg m², $J_{yy} = 5000$ kg m², $J_{zz} = 2000$ kg m², angular momentum of one GD rotor $h_{\text{rot}} = 20$ kg m²/s, GD damping coefficient $k_{3\beta_1, \beta_2} = 40$ N m / s², duration of deployment $T_f = 100\text{--}1000$ s.

The pantograph deployment essentially increases the components of the inertia tensor $\Theta_{1,1}^C$ and $\Theta_{2,2}^C$ and decreases slightly the component $\Theta_{3,3}^C$. Generally speaking, the inertia tensor is not a diagonal one in the presence of transverse design deviations along Ox axis. Because of transverse deviations, there is a nonzero component $\Theta_{1,3}$, but it is neg-

ligible small also as compared to the diagonal components of the inertia tensor and has no essential effect on the SC dynamics.

The increase in the inertia tensor components leads to the sharp decrease in the ω_2 magnitude (Figure 4) and to the SC orientation violation. Figure 5 shows how amplitude of ω_2 attenuate in the long-term consideration because of the GD operation.

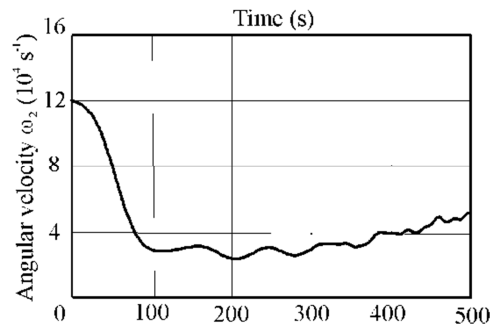


Figure 4. Time histories of absolute angular velocity projection ω_2

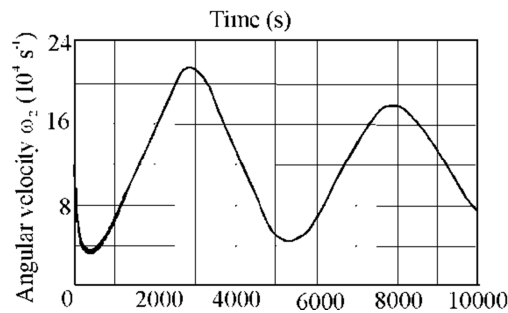


Figure 5. Time history of absolute angular velocity projection ω_2 in long-term consideration

At the same time, generalized co-ordinates $z_i (i=1,20)$ behave as it is shown in Figure 0. (Note that $z_i = z_{i,p}(t) + z_{i,e}$, where $z_{i,p}(t)$ are functions of time and $z_{i,e}$ are independent variables that determine elastic oscillations.) The dash lines correspond here to the usual deployment law, the solid lines – to the optimal law (Figure 0). This behaviour shows the appreciable longitudinal oscillations of the design at the deployment stage. Optimization of the deployment law reduces the vibration amplitudes considerably. The oscillating motions are induced by excitation of elastic oscillations of the design rods with the spring hinges. Their amplitudes grow with increase of the number of the tiers. Longitudinal oscillations have noticeable influence upon the components of the inertia tensor (Figure 4). In Figure 6 one may see that amplitude of oscillatory component of $z_{20,e}(\text{opt})$ is half of the same value for $z_{20,e}(\text{nonopt})$.

The transverse relative deviations of the design longitudinal axis that are defined by the generalized co-ordinates x_{20} are shown in Figure 7. Practically all these deviations are directed opposite to the vector of the SC velocity under the effect of the Coriolis forces.

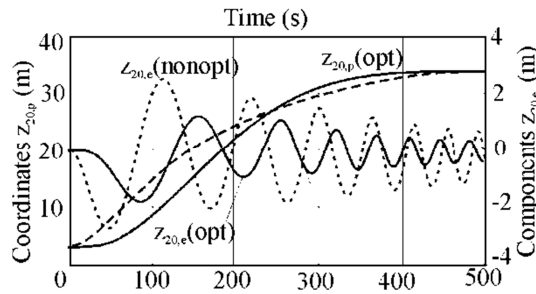


Figure 6. General coordinates z_{20} vs time

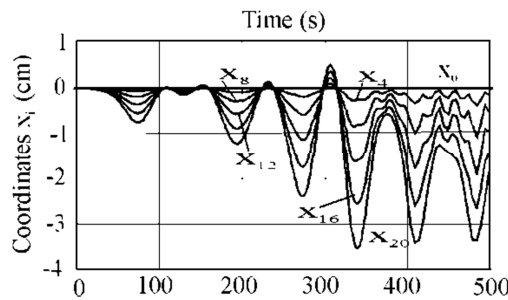


Figure 7. General coordinates x_i vs time

SC with switched off GD enters into a condition of simple harmonic pitch oscillations under the influence of the gravitational torque. Taking into account the Coulomb friction in design hinges practically has no influence on damping of these oscillations since elastic longitudinal oscillations of the design damp quickly enough. Transverse vibrations, on the contrary, damp very slowly as compared to deployment duration even under the influence of forces of structural damping since their amplitudes and velocities are very small as one can see in Fig. 7.

At twice as long deployment, the behaviour of the generalized co-ordinates becomes smooth enough; the oscillation amplitudes of overall design length do not exceed 0.15 m. The transversal deviations have a smooth mode. The design replicates the behaviour of a cantilever beam. The oscillating components are superimposed on these deviations. These deviations lead to a reduction of the amplitudes of vibration because of their strong connectedness with the pitch oscillations, which damp through the GD effect, even if the structural damping is not taken into consideration. At deployment of this design during 500 s from very heavy ideally stabilized space station, the amplitudes and frequencies of longitudinal and transversal oscillations visibly decrease.

The deviations of the GD angles $\tilde{\beta}_i$ during the stabilization process do not exceed 0.1 rad.

6. Conclusions

The present study deals with the exploration of the dynamics of the gyro-gravitational stabilized spacecraft in the mode of the deployment of the flexible pantograph structure. A novel mathematical model, computer simulations, new control profile for design deployment is presented. Novelty of the approach consists in the taking into account additional internal degrees of freedom of the pantograph design in comparison with known earlier settings of the problem; in using the developed by author method of derivation of the dynamic equations of mechanical systems with internal degrees of freedom and non-stationary connections; in using optimum with respect to damping of elastic oscillations control profile for deployment of flexible designs. A detailed simulation study has allowed to analyze the dynamic behaviour of the design at various values of parameters both the spacecraft with flexible pantograph structure and the laws of deployment. Data obtained permit the designer to select the most appropriate deployment, structure and gyro-dampers parameters. The results obtained from using the optimum control profile have been compared with those of the standard control profile. The comparison demonstrates that the proposed profile can significantly reduce the vibration of the flexible structure during deployment operations.

The developed computational FORTRAN code may be easily adopted for other deployed systems.

Acknowledgement

The author wishes to express his gratitude to Prof. V. S. Khoroshilov for his technical contributions in the work reported here.

References

1. V. Dranovskii, V. Khoroshilov, A. Zakrzhevskii, *Spacecraft dynamics with regard to elastic gravitational stabilizer deployment*, Acta Astronautica, **64** (2009) 501-513.
2. V. Khoroshilov, A. Kovalenko, A. Zakrzhevsky, *Dynamics of deployment of elastic pantograph designs on space vehicle*. XXII Symposium - Vibrations in physical systems – Poznań-Będlewo, (2006) 167- 172.
3. <http://www.vibsys.strefa.pl/journal/2006-22/167.pdf>
4. V. V. Beletsky, *Motion of an Artificial Satellite about its Center of Mass*, Israel Program for Scientific Translations, Jerusalem, 1966.
5. J. Awrejcewicz, *Classical Mechanics. Dynamics*, Springer-Verlag, New York, 2012.
6. A. I. Lurie, *Analytical mechanics*, Springer, 2002.
7. A. E. Zakrzhevskii, *Slewing of Flexible Spacecraft with Minimal Relative Flexible Acceleration*, J. of Guidance, Control, and Dynamics, **31** (2008) 563- 570.